Journal of Applied Polymer Science

Physicochemical and antibacterial properties of chitosan-polyvinylpyrrolidone films containing self-organized graphene oxide nanolayers

Nafiseh Mahmoudi,[1] Fatemeh Ostadhossein,[1] Abdolreza Simchi[1,2]

[1]Department of Materials Science and Engineering, Sharif University of Technology, Tehran 14588, Iran
[2]Institute for Nanoscience and Nanotechnology, Sharif University of Technology, Tehran 14588, Iran
Correspondence to: A. Simchi (E-mail: simchi@sharif.edu)

ABSTRACT: Chitosan films have a great potential to be used for wound dressing and food-packaging applications if their physicochemical properties including water vapor permeability, optical transparency, and hydrophilicity are tailored to practical demands. To address these points, in this study, chitosan (CS) was combined with polyvinylpyrrolidone (PVP) and graphene oxide (GO) nanosheets (with a thickness of ~1 nm and lateral dimensions of few micrometers). Flexible and transparent films with a high antibacterial capacity were prepared by solvent casting methods. By controlling the evaporation rate of the utilized solvent (1 vol % acidic acid in deionized water), self-organization of GO in the polymer matrix was observed. The addition of PVP to the CS/GO films significantly increased their water vapor permeability and optical transmittance. A blue shift in the optical absorption edge was also noticed. Thermal analysis coupled with Fourier transform infrared spectroscopy suggested that the superior thermal stability of the nanocomposite films was due to the formation of hydrogen bonds between the functional groups of chitosan with those of the graphene oxide. An improved bactericidal capacity of the nanocomposite films against gram-positive *Staphylococcus aureus* and gram-negative *Escherichia coli* bacteria was also observed. Highly flexible, transparent (opacity of 6.95), and antimicrobial CS/25 vol % PVP/1 wt % GO films were prepared. © 2015 Wiley Periodicals, Inc. J. Appl. Polym. Sci. **2016**, *133*, 43194.

KEYWORDS: biomaterials; films; graphene and fullerenes; nanotubes; polysaccharides

Received 2 February 2015; accepted 2 November 2015
DOI: 10.1002/app.43194

INTRODUCTION

The physical and structural properties of polymer films for biomedical and food-packaging applications have been studied frequently.[1–4] For these applications, biopolymers with tailored properties (for example, permeability, thermal stability, optical transparency, mechanical properties, and degradation rate) are desirable.[5,6] Chitosan (CS), which is obtained from the N-deacetylation of chitin, has promising properties including antimicrobial and antifungal activity, biocompatibility, biodegradability, high film forming ability, and low oxygen and carbon dioxide permeability.[7–13] It offers a versatile range of applications for drug delivery, hard and soft tissue engineering, wound dressing, and food packaging.[14–16] However, the wide application of CS is currently limited mainly because of relatively poor thermal stability, wet strength performance, darkening during storage at high temperatures, and UV degradation.[17–19] Therefore, many attempts have been performed on the synthesis and characterization of polyvinylpyrrolidone/chitosan (PVP/CS) films.[20,21] PVP is a biocompatible, nontoxic, hydrophilic and transparent synthetic polymer with a high film forming ability.[22–24] Strong interactions of carbonyl group of PVP with hydroxyl and amine groups of CS make them miscible with an improved light transparency and water vapor permeability.[21] However, the mechanical properties of PVP/CS films do not fulfill demands of many biomedical applications.[16,20,21] Therefore, some researchers have attempted to prepare CS-based nanocomposites containing reinforcing particles such as single-wall carbon nanotubes, Ag and TiO_2 nanoparticles.[4,7,9,16,25–27]

Graphene is a single layer of hexagonal carbon lattice with superior mechanical (high Young's modulus and hardness, and excellent flexibility), electronic and thermal properties.[28,29] Graphene oxide consists of graphene sheets which are chemically functionalized with hydroxyl, carbonyl and epoxy groups.[30,31] These functional groups provide strong interactions with polar solvents to form intercalated nanocomposites.[26] Experiments have also determined that GO nanosheets can potentially serve as a biocompatible, transferable, and implantable platform for

tissue regeneration and accelerated stem cell growth.[26,32] Additionally, GO sheets exhibit an antimicrobial activity against gram-positive and gram-negative bacteria.[26,32,33] Therefore, GO is a promising nanofiller for improving the properties of CS without hampering its biocompatibility. Epoxide, carboxyl, and hydroxyl groups present on the basal plane and edges of GO enable interactions with functional groups of CS; As a result, the strong H-bonding improves molecular level dispersion of GO sheets in the aquatic solvent of GO and CS.[34] Recent studies have revealed covalent-grafting of chitosan onto the surface of graphene nanosheets via amino bonds.[34,35] Improvement in the mechanical properties[34,36] and wettability[32] of CS by GO has also been reported. The biocompatibility of CS/GO composite films and their ability to promote human mesenchymal stem cell proliferation[32] have been shown as well.

Albeit the potential applications and advantages of GO-reinforced CS/PVP films for biomedicine and food-packaging applications, little work has been performed on their synthesis and characterizations. In the present work, flexible and transparent CS/PVP films containing GO nanosheets (1, 2, and 3 wt %) were prepared by a facile chemical procedure. Effects of PVP and GO on the water vapor permeability, optical transparency, hydrophilicity, thermal stability, and bactericidal capacity of CS films are presented. It is important to mention that hydrophilicity and permeability of composite films are very important parameters that control their biological performance. For instant, an intermediary range of permeability is often required for wound care materials. A high value of water permeability results in a dried wound area (which is not favorable for wound healing process) and a low value leads to the accumulation of exudates and subsequent decelerations of wound healing process by increased risk of bacterial growth.[1] Thermal stability is also important parameter to ease processing and sterilization. Therefore, the aim of this study was to investigate the physical properties and antibacterial capacity of CS/PVP/GO nanocomposite films.

MATERIALS AND METHODS

Chemicals

Chitosan ($M_w = 190 - 310$ kDa; degree of deacetylation: ~85%) and polyvinyl pyrrolidone (K-40, $M_w = 40$ kDa) were supplied by Sigma-Aldrich (Munich, Germany). Graphite powder was obtained from Qingdao Haida Graphite Co. (Qingdao, China, 99.8%). All other reagents ($NaNO_3$, $KMnO_4$, H_2SO_4, H_2O_2, nutrient agar, and acetic acid) were purchased from Merck KGaA (Darmstadt, Germany) with analytical grades.

Preparation of Graphene Oxide

Graphene oxide nanosheets were prepared from natural graphite by the modified Hummers' method.[37] Details of the chemical exfoliation procedure were explained elsewhere.[32] Briefly, 0.5 g graphite flakes were vigorously stirred for 10 min in 50 mL concentrated H_2SO_4 (98%) in an ice-water bath. Then, 0.5 g $NaNO_3$ and 3 g $KMnO_4$ were added into the solution dropwise and stirred for 2 h in the ice-water bath. After removing the bath, 100 mL deionized water (DI, Millipore, 18 MΩ) was slowly added into the suspension while the temperature was kept at 98°C. After stirring for 2 h, the temperature was reduced to 60°C and then 3 mL H_2O_2 (30 wt % aqueous solution) was added. The system was stirred until the absence of oxygen bubbles. Finally, the mixture was cooled to room temperature, diluted with DI water and left overnight. The obtained GO was filtered (grade No.40 filter paper, Whatman, Kent, UK) and washed with HCl (10 vol %) and DI water to remove the residual acid. GO sheets were obtained by sonication of the filtered product in DI water at power of 600 W (WiseClean,WUC-D10H, PMI-Labortechnik GmbH) for 1 h. The obtained dispersion was centrifuged 2 cycles at 5000 rpm for 20 min to remove unexfoliated GO.

Preparation of Nanocomposite Films

A chitosan solution was prepared by dissolving 1 g chitosan powder into acetic acid (98%) aqueous solution (of 1.0 vol %). The solution was stirred for 9 h at room temperature and then filtered (grade No.40 filter paper, Whatman, Kent, UK) to remove undissolved impurities. Separately, a PVP aqueous solution of 1.0 wt % was prepared by magnetic stirring for 7 h at room temperature. The solutions of CS and PVP were mixed at volume ratios of 75/25, 50/50, and 25/75 and stirred for 4 h. Then, the GO suspension (1.5 mg/mL) was slowly added into the CS/PVP solutions during a vigorous stirring. The concentration of GO was controlled to attain CS/PVP suspensions containing 1, 2 and 3 wt % GO (relative to the total dried weight of the polymer phase). The obtained solutions were agitated in an ultrasonic bath (WiseClean,WUC-D10H, PMI-Labortechnik GmbH) for 10 min at power of 600 W. Afterwards, the solution was stirred at ~35°C for 3 h and left overnight. The suspensions (ca. 37 mL) were then poured into 10 cm-diameter polystyrene Petri dishes with tight lids to provide slow evaporation. The lids had a small holes (~1 mm diameter). The suspensions were left to dry under a fume hood without air ventilation for 48 h.

Materials Characterization

Thickness Measurement. The thickness of films was measured by a digital micrometer (0.001 mm, Mitutoyo, Absolute Digimatic Japan). Ten measurements on each film were done and the average value with standard deviation was reported.

Scanning Electron Microscopy. The microstructure of the films was examined by a TESCAN scanning electron microscope (Czech Republic). The elastic films were grasped with forceps, frozen in a sink of liquid nitrogen, and bended by hand. The microstructure of the cross-section area was studied.

Hydrophilicity. Wettability of the films was measured by an OCA 15 plus video-based optical contact angle meter (Data Physics Instruments GmbH, Filderstadt, Germany). Four water droplets (4 μL each) were spread on the surface and the angles were analyzed by the device software.

Optical Properties. The transparency of the suspensions was examined by a 6705 UV-Vis spectrophotometer (Jenway, UK). The opacity of the films was determined by[38]:

$$\text{Opacity} = \text{Absorption at 600 nm}/\text{Film thickness (mm)} \quad (1)$$

Fourier Transform Infrared Spectroscopy. Fourier transform infrared (FTIR) spectrum of the films was determined in transmission mode by a ABB Bomem spectrometer (MB-100, Canada) in the range $400 - 4000$ cm^{-1} with a resolution of 4 cm^{-1}.

Atomic Force Microscopy. Atomic force microscopy (AFM, Auto Probe CP-Research-Veeco Instruments Inc., USA) was conducted to characterize the GO nanolayers in the tapping-mode. The patterns were scribed by using a 5 ×5 μm^2 piezo-electric scanner which could digitize the data into 1024 ×1024 pixels. The AFM tip was a pyramidal Si tip (NT-MDT NSG-10) with a tip radius of about 10 nm and an aspect ratio of about 1.2. The speed of the tip was 1 μm/s. The samples were prepared by dropping an aqueous GO solution (∼ 0.01 mg/mL) on a fresh silicon wafer.

Antibacterial Assay. Antibacterial activity studies were performed against Gram-negative *Escherichia coli* (ATCC, Code: 25922) and Gram-positive *Staphylococcus aureus* (ATCC, Code: 25923) bacteria using drop-test method.[39] The strains were supplied by the Biochemical and Bioenvironmental Research Institute (Tehran, Iran). The bacteria, which were in the exponential growth phase, were cultured in the nutrient broth (Merck KGaA, Darmstadt, Germany) at 37°C overnight. The cultured bacteria were diluted to reach approximately the concentration of 2.6 ×10^7 colony-forming unit (CFU) per ml. This concentration was confirmed by UV- Vis spectrometer (UV9200, BioTech Engineering, UK). The films were placed in sterilized Petri dishes after sterilizing by 70 vol % ethanol. Then, 100 µL of nutrient broth with bacteria was added dropwise onto the surface of the films. The samples were laid at ambient temperature for 12 h at 37°C. Afterwards, the numbers of surviving bacteria in the form of colony were counted on three specimens and the results were reported based on mean value with standard deviation.

Thermal Analysis. The thermal properties of the films were studied by differential scanning calorimetry (DSC, Q100, TA Instruments, and USA) at a heating rate of 10°C/min under a nitrogen atmosphere.

Permeability. Water vapor permeability was determined according to ASTM standard E 96-92. Briefly, each film was cut into the circles with 3 cm diameter and used to cover the glass permeation cups which contained 30 mL of DI water. The films were sealed tightly by the barrier tapes to ensure the prevention of any external materials transmission. The cups were placed in a desiccator and periodically weighted to inspect the water loss. The permeability was determined from the slope of weight loss-time (S) by[38]:

$$\text{Permeability} = S \times L/\Delta P \quad (2)$$

where L is the mean film thickness and ΔP the pressure difference between the two film sides. The pressure difference was determined from the humidity gradient (ΔR, the difference between the humidity of desiccant and water) and the saturation vapor pressure of water at the testing temperature ($P_0 = 35$ mmHg at 31.7°C) by:

$$\Delta P = P_0 \,.\, \Delta R \quad (3)$$

RESULTS AND DISCUSSION

Morphology and Structure of Nanocomposite Films

Figure 1(a) shows an AFM image of chemically exfoliated GO sheets prepared by the modified Hammer's method. The height histogram along Line 1 [Figure 1(a)] is illustrated in Figure 1(b). The height difference between two points along Line 1 [Figure 1(c)] indicated that the GO sheets had a thickness of ∼0.9 nm with lateral dimensions of few micrometers. As compared with the mono-layer GO sheets with a thickness of 0.34 nm,[32,35] the GO sheets were composed of a few layers.

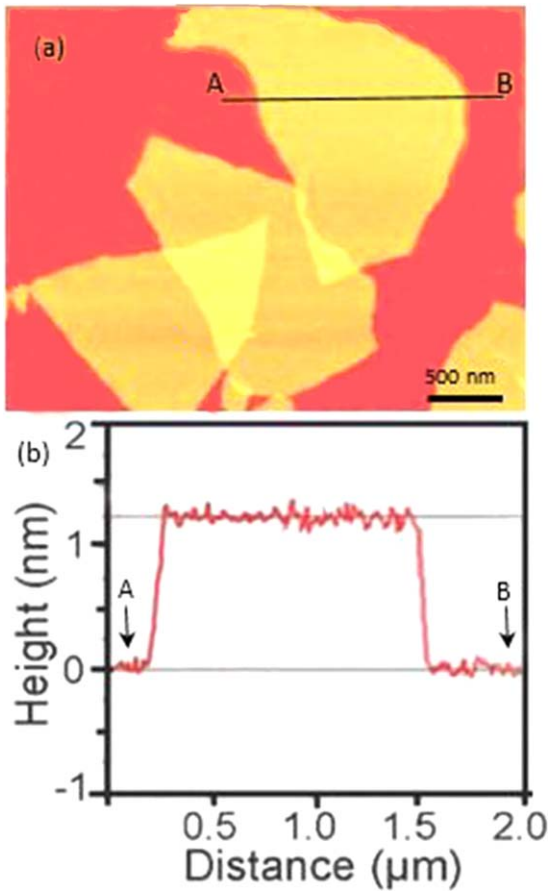

Figure 1. (a) AFM image, (b) height histogram along line 1 shown in image and (c) height profile of graphene oxide nanosheets. [Color figure can be viewed in the online issue, which is available at wileyonlinelibrary.com.]

SEM investigation was employed to study the configuration of the GO nanosheets in the polymer matrix. Figure 2 shows typical SEM images of the CS films containing GO sheets. The top-view image of the CS/PVP film indicated a relatively smooth surface without defects [Figure 2(a)]. The addition of 1 wt % GO increased the surface roughness while the nanosheets appeared to protrude from the polymer matrix [Figure 2(b)]. A fined-wrinkled surface with more organized structure was attained at the high concentration of GO nanosheets [Figure 2(c)].Cross-sectional SEM study showed an embedded structure of the GO layers in the polymer matrix with very rough surface [Figure 2(d)].

FTIR spectra of the CS/PVP films containing 1 wt % GO are shown in Figure 3(a). The CS absorption peaks are located at 1073, 1595, and 1649 cm^{-1} which correspond to the stretching vibration of C—O, the deformation bending of N—H and the stretching vibration of both C═O, and the C—N of amide group, respectively.[36,40] The IR peak at 3400 cm^{-1} is assigned to the

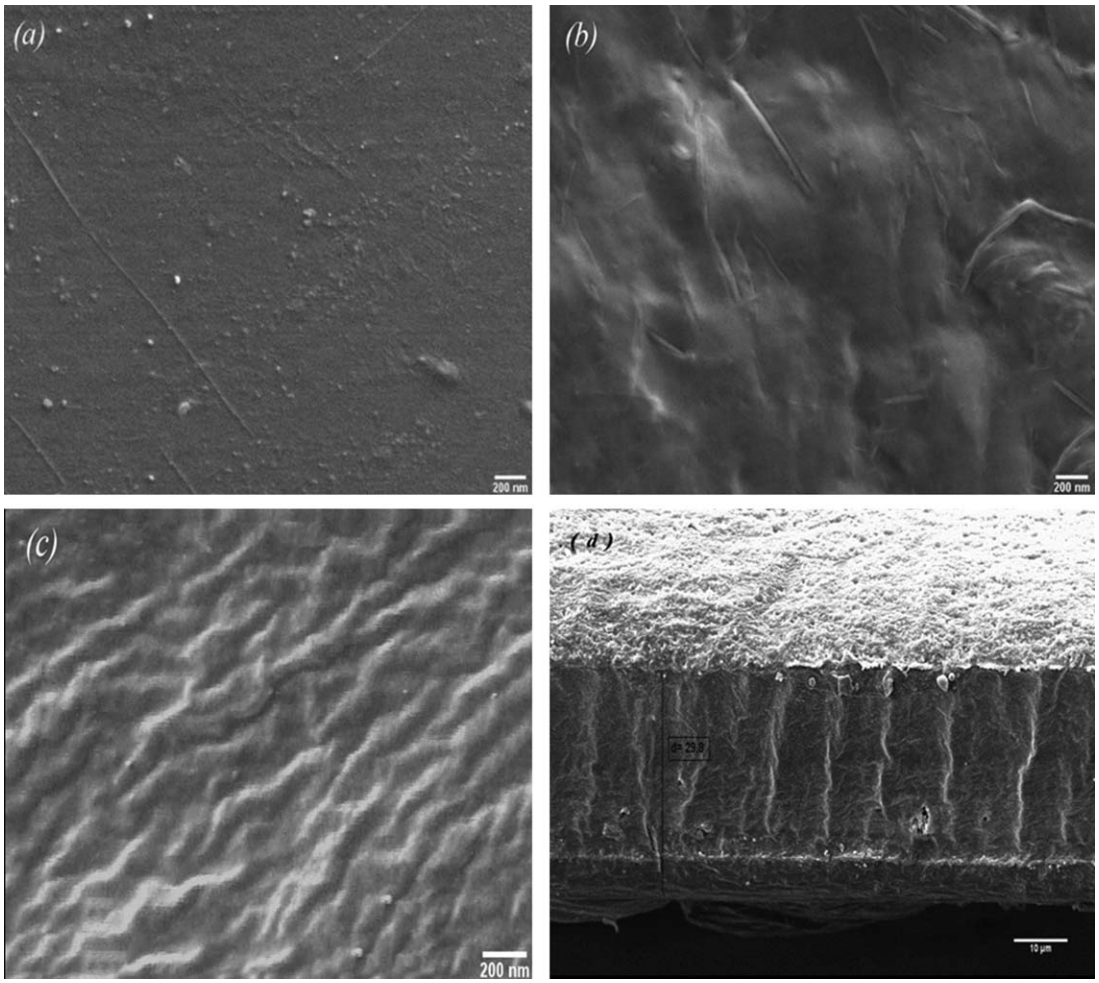

Figure 2. SEM micrographs of the chitosan-based films: (a) CS-25 vol % PVP film; (b) CS-25 vol % PVP-1 wt % GO; (c) and (d) CS-25 vol % PVP-3 wt % GO; (a-c) top-view SEM images and (d) a cross-sectional SEM image.

intermolecular hydrogen bonding between hydroxyl and amino groups in CS. The PVP absorption peaks are seen at 1285, 1375, 1458, and 1663 cm^{-1} (amide I, C═O and C—N groups). The characteristic peaks of GO are located at 1057, 1379, 1614, 1726, and 3147 cm^{-1} which are attributed to C—O (epoxy), O—H (carboxyl), C—C assigned to skeletal vibrations of unoxidized graphite domains, C═O in carboxylic acid and carbonyl moieties, and O—H (hydroxyl), respectively.[35,41] In the CS/PVP film, interactions between proton-donor (protonated) groups of CS such as OH-C_6, OH-C_3, and NH_2-C_2, and the proton- acceptor functional group of C═O in PVP are feasible.[17] Nevertheless, OH-C_6 and OH-C_3 are more likely to form hydrogen boding (compared with NH_2-C_2) due to their higher intrinsic polarity.[16,20] Ordikhani *et al.*[42] and Mazaheri *et al.*[32] have recently shown that hydrogen bonding between functional groups of CS and carbonyl and epoxy groups of GO is susceptible. Therefore, the possible interactions between the constituents in the nanocomposite film can schematically be shown in Figure 3(b).

Flexibility and Transparency

Figure 3(c) shows UV-Vis absorption spectra of CS/GO (1 wt %) suspensions containing various amounts of PVP. The strong absorption peak at around 220 − 230 nm is attributed to π-π^* transitions in C—C aromatic bonds.[43] The change in the slope (shoulder) at 300 nm can also be related to π-π^* transitions in C—O bonds.[31,43] As the concentration of PVP increases, a decrease in the peak intensity with a slight blue shift in the absorption wavelength is seen. From eq. (1), the opacity of the films was determined (see Table I). The results indicate that at a constant GO content, the addition of PVP decreases the opacity of CS films, i.e., the films become more transparent. In contrast, at a constant PVP concentration, the GO sheets increase the opacity of the CS/PVP films. As Figure 3(d) shows, the addition of GO causes a color shift from colorless and yellowish to light brown. It is known that the absorption coefficient of graphene materials varies with their lateral size distribution, the mean number of layers per flake and their functional groups.[44] Since the exfoliated GO sheets are multilayer (Figure 2) and stacked in self-organized manner in the polymer matrix (Figure 1), they absorb more light than monolayer graphene. Therefore, the transparency of the nanocomposite films is significantly reduced when a high concentration of GO is loaded. Anyway, the transparency of the composite film containing 1 wt % GO is still maintained at a favorable level [Figure 3(d)] while the film is highly flexible.

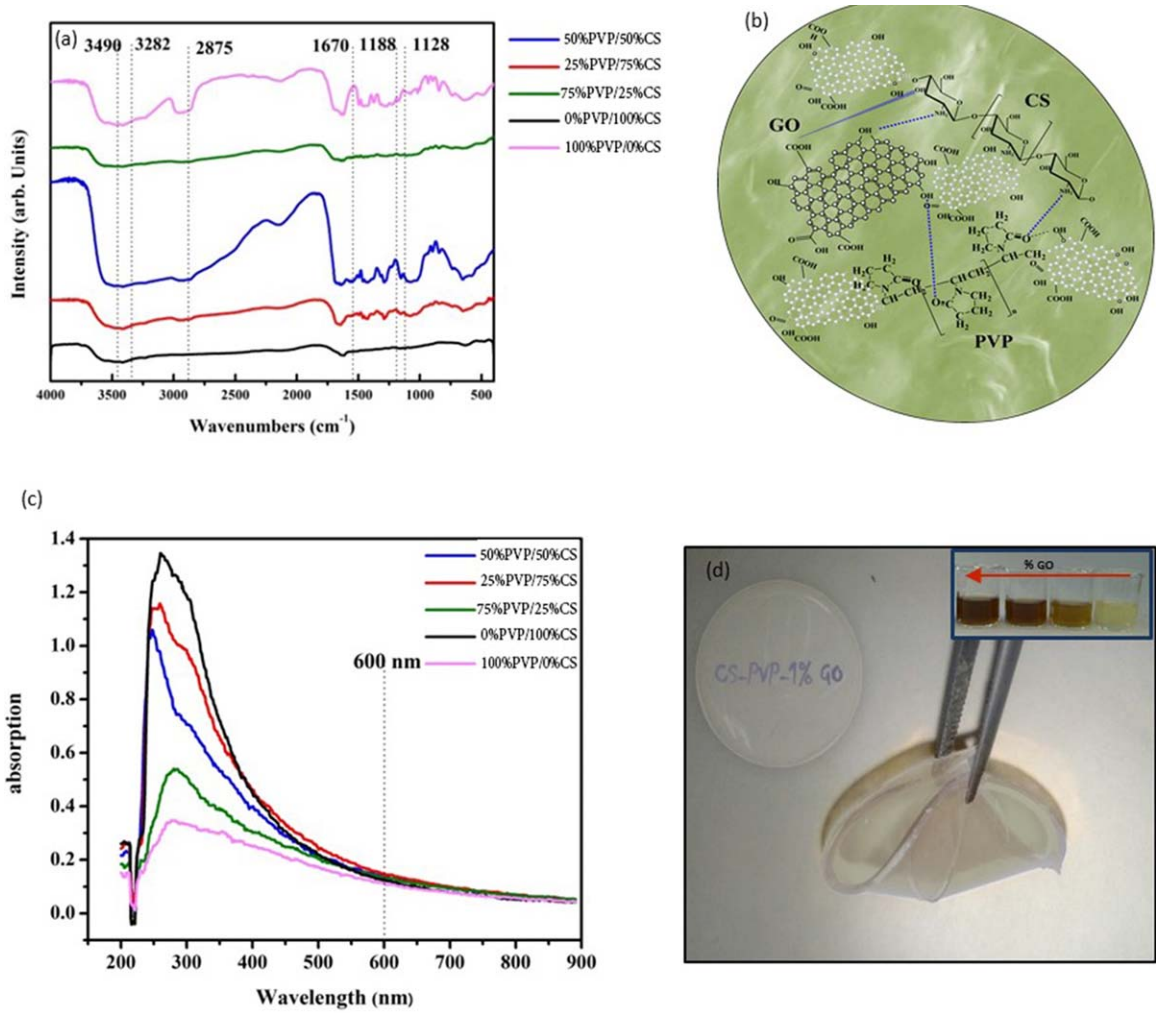

Figure 3. (a) FTIR spectra of CS-PVP films containing 1 wt % GO nanosheets. (b) Schematic intermolecular hydrogen bonding between polymer chains and GO. (c) UV-Vis spectra of CS-PVP films containing 1 wt % GO nanosheets. (d) Digital image of a flexible transparent CS-25 vol % PVP-1 wt % GO film. The insert in (d) shows digital images of CS-25 vol % PVP suspensions containing different amounts of GO. [Color figure can be viewed in the online issue, which is available at wileyonlinelibrary.com.]

Permeability and Hydrophilicity

Effects of PVP and GO addition on the wettability and water vapor permeability of the films are shown in Figure 4. The results showed that the PVP addition decreased the hydrophobicity of CS films [Figure 4(a)] mainly due to the hydrophilic amino and carboxylic groups of PVP.[25] The GO nanosheets also decreased the hydrophobicity of CS [Figure 4(b)]. On the other hand, permeability measurements indicated that the permeability highly depended on the PVP concentration [Figure 4(c)]. The high intrinsic permeability of PVP is due to its pyrrolidone ring-form morphology[21] which acts as a tunnel to let H_2O molecular diffuse through it. The addition of GO decreased the

Table I. Results of Thermal Analysis for CS-1%GO Films Containing Different Amounts of PVP

GO content (%)		0		1		2	
PVP content (%)	thickness (μm)	Absorption	Opacity	Absorption	Opacity	Absorption	Opacity
0	30 ± 8	0.202	6.73	0.213	7.1	0.230	7.66
25	22 ± 4	0.142	6.45	0.153	6.95	0.186	8.45
50	30 ± 8	0.117	3.9	0.127	4.23	0.147	4.9
75	24 ± 5	0.089	3.7	0.097	4.04	0.116	4.83
100	27 ± 5	0.072	2.66	0.113	4.18	0.110	4.07

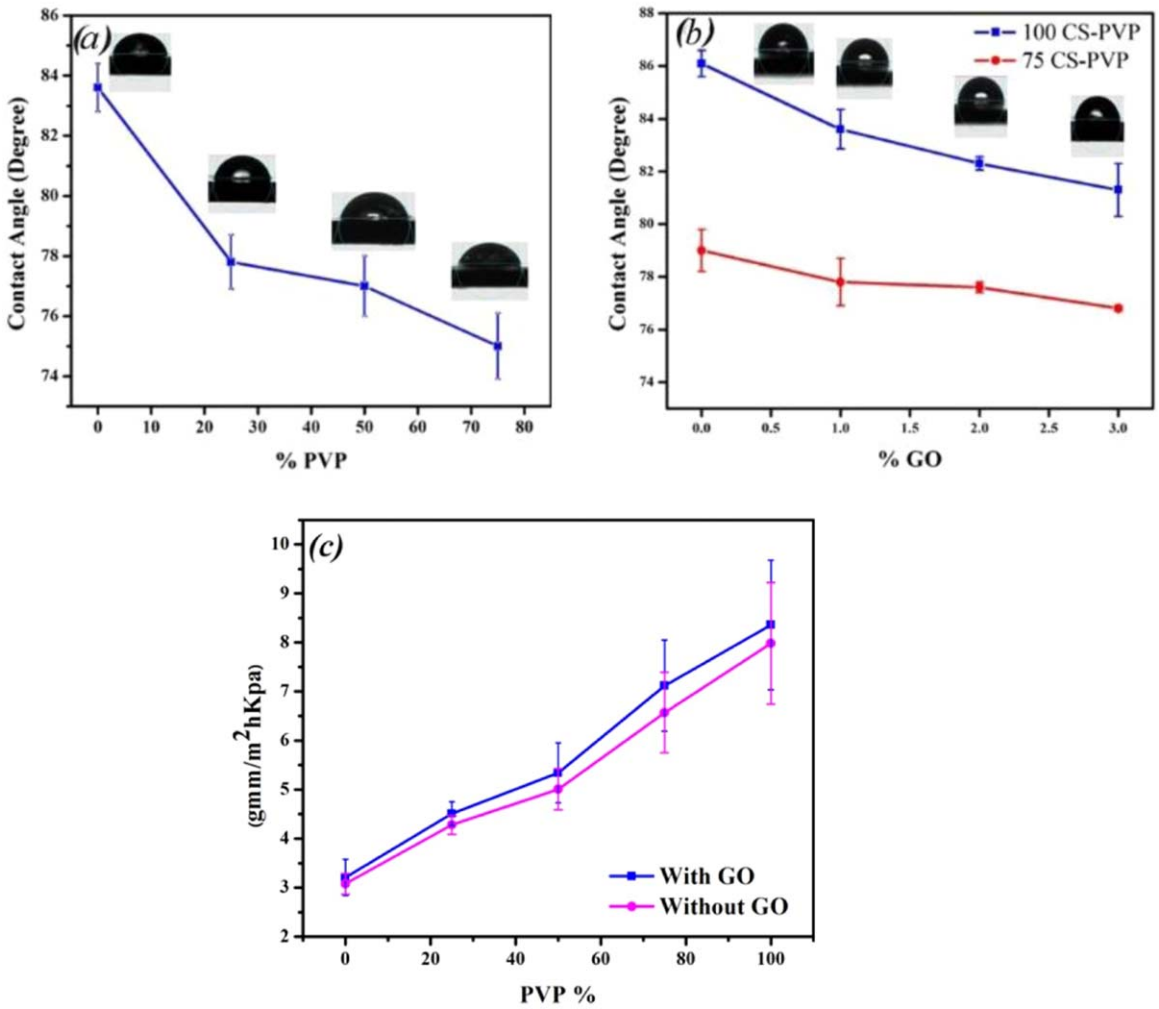

Figure 4. Effect of (a) PVP concentration and (b) GO content on the water contact angle of chitosan films. (c) Effect of 1 wt % GO addition on the permeability of CS/PVP films. [Color figure can be viewed in the online issue, which is available at wileyonlinelibrary.com.]

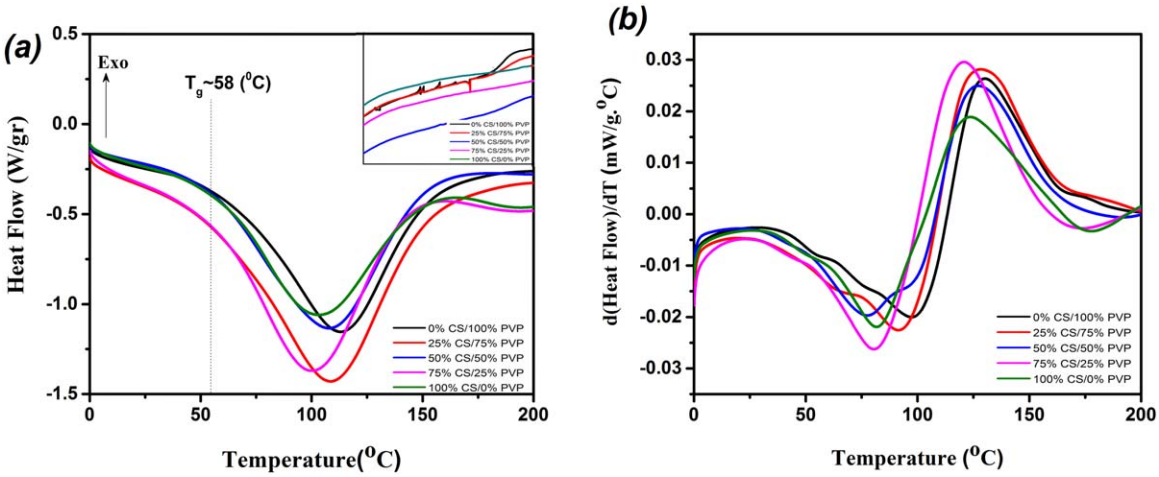

Figure 5. Thermal analysis of chitosan-based films containing 1 wt % GO. (a) DSC traces dependent on the PVP content. The inset shows the traces after cooling. (b) Derivate of heat flow versus temperature. [Color figure can be viewed in the online issue, which is available at wileyonlinelibrary.com.]

Table II. Effect of GO and PVP Concentration on the Absorption (at 600 nm) and Opacity of CS Films

	Heating cycle		Cooling cycle	
PVP content (%)	T_g (°C)	Peak temperature (°C)	Heat Flow (J/g)	Peak temperature (°C)
0	61.4	104	7.1	135
25	56.1	101	7.1	150
50	57.9	109	4.2	159
75	59.4	110	4.0	161
100	65.4	114	4.18	163

water vapor permiability. The high aspect ratio of the GO sheets and their self-organization in the polymer matrix could impede the diffusion of the water molecules.

Thermal Stability

Figure 5(a) shows DSC traces for the CS/PVP/GO (1 wt %) films. In order to indicate the glass transition temperature (T_g), the derivate of DSC traces are shown in Figure 5(b). The key temperature points in the DSC analysis are summarized in Table II. The presence of a single T_g for different composites indicates the complete miscibility of the different components.[23] During the heating cycle, endothermic peaks at around 100°C are ascribed to the structural water loss. A change in the slope of the curves on cooling represents the onset temperature of heat tolerance (see the inset). From these results, it was concluded that the addition of PVP slightly shifted up the glass transition temperature as well the peak temperature. It was suggested that molecular interactions between amino and carboxylic groups of CS, PVP, and GO changed the bond strength and improved the thermal stability.

Antibacterial Potential

The colony counting method was used to evaluate bactericidal capacity of the films against gram positive *S. aureus* and gram-negative *E. coli* bacteria. Figure 6 shows the effect of PVP and GO addition on the antimicrobial activity of CS. The pristine CS film (without PVP and GO) exhibited moderate antibacterial potential (~85% reduction in the bacteria colony). The antimicrobial properties of CS are related to interactions between cationic moieties of CS with ionic groups on the cell surface.[45] These interactions increase intercellular protein leakage and enzyme inhibition via chelating transition metals. The CS/PVP films exhibited a slightly lower bactericidal potential than pristine CS. Note that PVP have no antimicrobial activity.[21] The results also indicated an improved bactericidal capacity of the films in the presence of GO. The main mechanism responsible for the antibacterial effects of GO is the direct (physical) interaction between the sharp edges of the GO sheets and the bacterial cell membrane as well as oxidative stress.[26] Since the concentration of GO nanosheets in the polymer matrix was relatively low (≤3 wt %), their effect on the antimicrobial activity was not very pronounced. The results also indicated that the films containing GO had a much stronger antibacterial effect on *S. aureus* than *E. coli*, in good agreement with previous studies.[32] This could be attributed to the electron affinity between opposite charges present on bacterial cell wall and GO sheets.[32] The *S. aureus* bacterium is also more sensitive to the direct contact interaction of the graphene sheets than Gram-negative *E. coli*.

CONCLUSIONS

Chitosan-based films containing various amounts of PVP (up to 50 vol %) and GO (1 − 3 wt %) were prepared by solvent casting methods. The nanocomposite films showed tunable optical properties and permeability dependent on the concentration of PVP and GO. The physical and antibacterial properties of the films were studied. Self-organization of GO nanosheets in the CS/PVP matrix was noticed. FTIR spectroscopy revealed interactions between amino and carboxylic groups of the composite blends. Consequently, the thermal stability of CS films was improved. It was also shown that the addition of PVP and GO nanosheets enhanced the hydrophilicity and water permeability of the CS films. The CS film containing 25 vol % PVP and 1 wt % GO exhibited high transparency (Opacity = 6.95) and flexibility. This film also exhibited a high antimicrobial capacity due to inherent bacterial capacity of CS and the effect of GO nanosheets on the bacteria viability. The antimicrobial activity was stronger on *S. aureus* than *E. coli*.

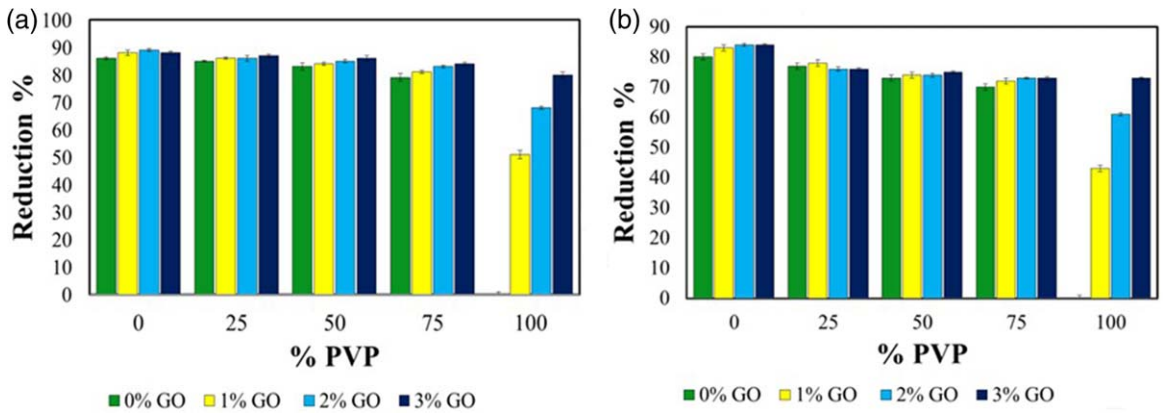

Figure 6. Antimicrobial activity of chitosan-based films dependent on the PVP content and GO concentration against (a) *S. aureus* and (b) *E. coli*. [Color figure can be viewed in the online issue, which is available at wileyonlinelibrary.com.]

ACKNOWLEDGMENTS

The authors acknowledge Dr. Tayebeh Gheiratmand, Mrs. Azade Rohani, Mr. Eng. Amin Jalali, and Mr. Eng. Mohammad Mahdi Mozaffar (Sharif University of Technology) for experimental and technical support. AS thanks funding support from the Grant Program of Sharif University of Technology (No. G930305) and Elite National Institute.

REFERENCES

1. Kim, I.-Y.; Seo S.-J.; Moon, H.-S.; Yoo, M.-K.; Park, I.-Y.; Kim, B.-C.; Cho, C.-S. *Biotechnol. Adv.* **2008**, *26*, 1.
2. Jayakumar, R.; Prabaharan, M.; Sudheesh Kumar, P.; Nair, S.; Tamura, H. *Biotechnol. Adv.* **2011**, *29*, 322.
3. Razzak, M. T.; Darwis, D. *Radiat. Phys. Chem.* **2001**, *62*, 107.
4. Rhim, J. W.; Park, H.-M.; Ha, C.-S. *Prog. Polym. Sci.* **2013**, *38*, 1629.
5. Siracusa, V.; Rocculi, P.; Romani, S.; Rosa, M. D. *Trends Food Sci. Technol.* **2008**, *19*, 634.
6. Roy, N.; Saha, N.; Kitano, T.; Saha, P. *Carbohydr. Polym.* **2012**, *89*, 346.
7. Rhim, J.-W.; Hong, S.-I.; Park, H.-M.; Ng, P. K. *J. Agricultural Food Chem.* **2006**, *54*, 5814.
8. Dutta, P.; Tripathi, S.; Mehrotra, G.; Dutta, J. *Food Chem.* **2009**, *114*, 1173.
9. Cruz-Romero, M.; Murphy, T.; Morris, M.; Cummins, E.; Kerry, J. *Food Control* **2013**, *34*, 393.
10. Tikhonov, V. E.; Stepnova, E. A.; Babak, V. G.; Yamskov, I. A.; Palma-Guerrero, J.; Jansson, H.-B.; Lopez-Llorca, L. V.; Salinas, J.; Gerasimenko, D. V.; Avdienko, I. D. *Carbohydr. Polym.* **2006**, *64*, 66.
11. Xu, J.; McCarthy, S. P.; Gross, R. A.; Kaplan, D. L. *Macromolecules* **1996**, *29*, 3436.
12. Park, J. H.; Cho, Y. W.; Chung, H.; Kwon, I. C.; Jeong, S. Y. *Biomacromolecules* **2003**, *4*, 1087.
13. Peelman, N.; Ragaert, P.; De Meulenaer, B.; Adons, D.; Peeters, R.; Cardon, L.; Van Impe, F.; Devlieghere, F. *Trends Food Sci. Technol.* **2013**, *32*, 128.
14. Bansal, V.; Sharma, P. K.; Sharma, N.; Pal, O. P.; Malviya, R. *Adv. Biol. Res.* **2011**, *5*, 28.
15. Nacer Khodja, A.; Mahlous, M.; Tahtat, D.; Benamer, S.; Larbi Youcef, S.; Chader, H.; Mouhoub, L.; Sedgelmaci, M.; Ammi, N.; Mansouri, M. B. *Burns* **2013**, *39*, 98.
16. Archana, D.; Singh, B. K.; Dutta, J.; Dutta, P. *Carbohydrate Polymers* **2013**.
17. Yeh, J. T.; Chen, C. L.; Huang, K.; Nien, Y.; Chen, J.; Huang, P. *J. Appl. Polym. Sci.* **2006**, *101*, 885.
18. Wasikiewicz, J. M.; Yoshii, F.; Nagasawa, N.; Wach, R. A.; Mitomo, H. *Radiat. Phys. Chem.* **2005**, *73*, 287.
19. Sarasam, A. R.; Krishnaswamy, R. K.; Madihally, S. V. *Biomacromolecules* **2006**, *7*, 1131.
20. Zeng, M.; Xiao, H.; Zhang, X.; Sun, X.; Qi, C.; Wang, B. *J. Macromol. Sci. Part B* **2011**, *50*, 1413.
21. Li, J.; Zivanovic, S.; Davidson, P.; Kit, K. *Carbohydr. Polym.* **2010**, *79*, 786.
22. Nie, W.; Yu, D.; Branford-White, C.; Shen, X.; Zhu, L. *Mater. Res. Innovat.* **2012**, *16*, 14.
23. Bernal, A.; Kuritka, I.; Saha, P. *J. Appl. Polym. Sci.* **2013**, *127*, 3560.
24. Rosiak, J.; Ulański, P.; Pajewski, L.; Yoshii, F.; Makuuchi, K. *Radiat. Phys. Chem.* **1995**, *46*, 161.
25. Yu, D.-G.; Shen, X.-X.; Branford-White, C.; White, K.; Zhu, L.-M.; Bligh, S. A. *Nanotechnology* **2009**, *20*, 055104.
26. Liu, S.; Zeng, T. H.; Hofmann, M.; Burcombe, E.; Wei, J.; Jiang, R.; Kong, J.; Chen, Y. *ACS Nano* **2011**, *5*, 6971.
27. Vecitis, C. D.; Zodrow, K. R.; Kang, S.; Elimelech, M. *ACS Nano* **2010**, *4*, 5471.
28. Mukhopadhyay, P.; Gupta, R. K. *Plast. Eng.* **2011**, *32*, 67.
29. Ramanathan, T.; Abdala, A.; Stankovich, S.; Dikin, D.; Herrera-Alonso, M.; Piner, R.; Adamson, D.; Schniepp, H.; Chen, X.; Ruoff, R. *Nat. Nanotechnol.* **2008**, *3*, 327.
30. Hu, X.; Mu, L.; Wen, J.; Zhou, Q. *Carbon* **2012**, *50*, 2772.
31. Chaiyakun, S.; Witit-Anun, N.; Nuntawong, N.; Chindaudom, P.; Oaew, S.; Kedkeaw, C.; Limsuwan, P. *Procedia Eng.* **2012**, *32*, 759.
32. Mazaheri, M.; Akhavan, O.; Simchi, A. *Appl. Surf. Sci.* **2014**, *301*, 456.
33. Lim, H. N.; Huang, N. M.; Loo, C. *J. Non-Crystalline Solids* **2012**, *358*, 525.
34. Han, D.; Yan, L.; Chen, W.; Li, W. *Carbohydr. Polym.* **2011**, *83*, 653.
35. Pan, Y.; Wu, T.; Bao, H.; Li, L. *Carbohydr. Polym.* **2011**, *83*, 1908.
36. Zuo, P.-P.; Feng, H.-F.; Xu, Z.-Z.; Zhang, L.-F.; Zhang, Y.-L.; Xia, W.; Zhang, W.-Q. *Chem. Central J.* **2013**, *7*, 39.
37. Hummers Jr., W. S.; Offeman, R. E. *J. Am. Chem. Soc.* **1958**, *80*, 1339.
38. Abdollahi, M.; Alboofetileh, M.; Behrooz, R.; Rezaei, M.; Miraki, R. *Int. J. Biol. Macromol.* **2013**, *54*, 166.
39. Esfandiari, N.; Simchi, A.; Bagheri, R. *J. Biomed. Mater. Res. A* **2014**, *102*, 2625.
40. Fan, H.; Wang, L.; Zhao, K.; Li, N.; Shi, Z.; Ge, Z.; Jin, Z. *Biomacromolecules* **2010**, *11*, 2345.
41. Guo, H.-L.; Wang, X.-F.; Qian, Q.-Y.; Wang, F.-B.; Xia, X.-H. *ACS Nano* **2009**, *3*, 2653.
42. Ordikhani, F.; Farani, M. R.; Dehghani, M.; Tamjid, E.; Simchi, A. *Carbon* **2015**, *84*, 91.
43. Lai, Q.; Zhu, S.; Luo, X.; Zou, M.; Huang, S. *AIP Adv.* **2012**, *2*, 032146.
44. Sun, B.; Long, Y. Z.; Zhang, H. D.; Li, M. M.; Duvail, J. L.; Jiang, X. Y.; Yin, H. L. *Prog. Polym. Sci.* **2014**, *39*, 862.
45. Sudarshan, N.; Hoover, D.; Knorr, D. *Food Biotechnol.* **1992**, *6*, 257.